

Seismic behavior of irregular RC-Frames damaged by corrosion

Stefania Imperatore

Department of Civil Engineering, Nicolò Cusano University, Rome, Italy

Mahdi Kioumarsi

Department of Civil Engineering and Energy Technology, Oslo Metropolitan University, Oslo, Norway

ABSTRACT: Reinforced concrete (RC) structures frequently are deteriorated by corrosion attack where pitting morphology is the worst form of degradation. Appropriate vulnerability analyses, accounting for the variation of mechanical properties of material during the time, give an assessment of the residual service life of corroded structures. Aim of the present paper is to evaluate any variation in the seismic behaviour of an irregular poor-designed RC frame subjected to the chloride attack. The progressive stiffness degradation and the effects of higher modes are considered in the study by means of displacement-based adaptive pushover analyses.

1 INTRODUCTION

The use of reinforced concrete (RC) in residential structures dates back the late nineteenth century, but its maximum expansion is reached after the Second World War. In this age, the RC material was considered almost invulnerable and then the problems related to durability were disregarded. Residential buildings realized between the 1950 and the 1980 are characterized by low quality materials (smooth or slightly-ribbed steel with poor mechanical properties and low-strength concretes) and limitation in the constructive details. In particular, too little attention was paid to the thickness of concrete cover that nowadays, is instead proportionated to the environmental aggressiveness. As a results, corrosion degradation is set to become more prevalent and then a proper definition of the residual performance of deteriorated RC structures is required (Zanini et al., 2016 and 2017; Bossio and Bellucci, 2019).

The main forms of degradation in reinforced concrete structures are related to carbonation and chloride attack. In the first case, the aggressive agent is CO₂, which permeates inside the concrete with a speed that depends on concrete strength and porosity, carbon dioxide concentration, humidity level and ambient temperature. In chloride attack, the degradation is caused by chloride ions that run through the environments (marine structures or viaducts treated with deicing salts) or are inside raw materials as contami-

nant agent. In each case, the alkalinity level of reinforcements is reduced, the iron is no longer in the passivation phase and corrosion occurs (uniform or localized as a function of the corrosion potential and pH variation).

Analytical, numerical and experimental studies have shown that the reinforcements' corrosion induces:

- cracking and bond-strength reductions (Andrade et al., 1993; Coronelli, 2002; Vidal et al., 2004; Zhang et al, 2010; Coccia et al., 2016; Bossio et al., 2015 and 2017);
- reduction of the reinforcement cross-section, and mechanical properties decay (Apostolopoulos and Papadopoulos, 2007; Apostolopoulos et al., 2013; Kashani et al, 2013a and 2013b; Imperatore et al., 2017);
- ductility and load-bearing capacity reduction (Rodriguez et al., 1997; Vu and Stewart, 2000; Vidal et al., 2007, Zandi Hanjari et al, 2011; Imperatore et al., 2012 and 2016; Kioumarsi et al., 2014-2017).

All these aspects are principally referred to structural performance under static loads, where unfortunately the seismic issue is still little addressed. However, occurred earthquakes in the last decades highlighted the high vulnerability of structures realized in the post-WWII (Baiocchi et al., 2012; Ferlito et al., 2013; Romano et al., 2018), often subjected also to degradation phenomena, related to the ageing

and the environmental exposition, that cause the reinforcements' corrosion.

The performance of structures affected by chloride attack is an issue typically referred to infrastructures treated with deicing salts: the effects of a strongly localized corrosion and the related structural problems are nowadays evident. However, number of cases of buildings which significantly damaged by corrosion begin to grow, and then the problem should be addressed by a seismic perspective as well. Interesting food for thoughts on the seismic response of corroded building can be found in (Berto et al., 2012; Inci et al., 2012; Bossio et al., 2018 and 2019), where the issue is approached according to simplified models. Nevertheless, even some degradation's aspects are disregarded, the overall decay in terms of strength, ductility and seismic capacity is clear.

The aim of this paper is to evaluate the seismic performance of RC structures subjected to different corrosion scenarios by chloride attack, which, according to the opinion of the authors, represents the deterioration phenomenon characterized by higher risk. The study focus on the behavior of multi-storey RC frame building, irregular in elevation and designed according to the criteria compatible with a structural age congruent with the considered corrosion level. To account for the safety level variation and the residual life of the analyzed structure, both the corrosion trigger time and the service life as a function of the corrosion rate should be accurately defined. Moreover, the mechanical properties decay of corroded reinforcements, and the consequent confinement reduction, are considered in the model; cracking and bond-slip law variations are instead disregarded because the chloride attack produces a localized corrosion, a degradation morphology that doesn't mix well with a global performance decay induced by a generalized bond deterioration.

2 EFFECTS OF THE CHLORIDE ATTACK ON THE STEEL REINFORCEMENT

When a certain critical content of chloride ions is achieved on the steel reinforcements, the chloride attack, one of the most dangerous cause of degradation, is triggered. In civil infrastructures (bridges and viaducts), chloride attack is quite widespread due to the massive use of thawing salts, which cause a corrosion characterized by deep pits in the reinforcements' curbs and columns caps accompanied by extensive phenomena of spalling of the concrete cover. On the other hand, in RC buildings, the corrosion is related to the transport and deposition of salts in the marine environment and can occur even without clear degradation signs; in particular, a low-alkaline concrete exposed to the atmosphere may suffer of chloride attack in presence of relatively low chloride content.

The chlorides diffusion law in the space, has been defined only in a simplified way (Meira et al., 2008),

accounting only for the salinity at the waterline and disregarding the other several characterizing variables (wind, humidity, temperature, chlorides distribution on both the ground and the structure, etc.)

Experimental studies on the deposition of marine aerosols in samples placed at different distances from the sea (Lindvall, 2007; de Rincon et al., 2007; Adam et al., 2016; Meira et al. 2017) provide values of the superficial chlorides concentration (hereinafter defined C_s), a parameter that allows to evaluate the corrosion initiation time. The values assumed by C_s are extremely variable and it is very difficult to define it uniquely. On buildings exposed to the marine environment, the superficial chloride concentrations vary between 0.09% and 0.85% (Medeiros et al., 2013; Moreno et al., 2015), depending on the exposure conditions, the salts concentration, the concrete strength and porosity.

In the concrete, chloride ions diffuse with a decreasing concentration profile, typically studied with the second Fick's law (fib, 2006):

$$C(x, t) = C_s \cdot \left[1 - \operatorname{erf} \left(\frac{x}{2 \cdot \sqrt{D_{app}(t) \cdot t}} \right) \right] \quad (1)$$

where $C(x, t)$ represents the total chloride content (as percentage of the concrete or cement weight) at the time t and at the distance x from the surface, while D_{app} (cm²/sec) is the chloride diffusion speed, defined as:

$$D_{app}(t) = k_e \cdot D_{RCM0} \cdot k_t \cdot A(t) \quad (2)$$

wherein:

- k_e is an environmental parameter defined as:
- $$k_e = \exp \left[5500 \cdot \left(\frac{1}{T_{ref}} - \frac{1}{T_{real}} \right) \right]$$
- T_{ref} is the reference temperature (293K),
 - T_{real} the ambient temperature (K)
 - D_{RCM0} is the chloride migration coefficient (15.8 μm²/s)
 - k_t is an experimental parameter fixed equal to 1 in the absence of any further benchmarks;
 - $A(t)$ is an ageing function defined as:

$$A(t) = \left(\frac{t_0}{t} \right)^a$$

where t_0 is the concrete curing duration and a is related to the structural age.

When, on the reinforcement surface, a certain chloride content (the critic chloride content, C_{cr}) is reached, the corrosion process can start. The parameter C_{cr} depends on several factors (superficial chlorides concentration, concrete properties, concrete cover thickness, humidity, temperature, etc.). Assuming that the chlorides penetration is a diffusive process that varies in time, the initiation corrosion period may be estimated as the instant T_i in which critical chloride content (C_{cr}) is reached.

Once that T_i has been evaluated, the corrosion process develops with a certain rate, to properly define as a function of the environmental conditions. According to (Val and Melchers, 1997), the steel consumption due to the pitting corrosion at time t , can be estimated as:

$$p(t) = 0.0116 \cdot i_{corr}(T_i) \cdot R_p \cdot (t - T_i) \quad (3)$$

where i_{corr} is the equivalent corrosion current density, depending by concrete resistivity (Andrade et al., 2002; Liu and Weyers, 1996 and 1998) and environmental conditions (Rodriguez et al., 2006).

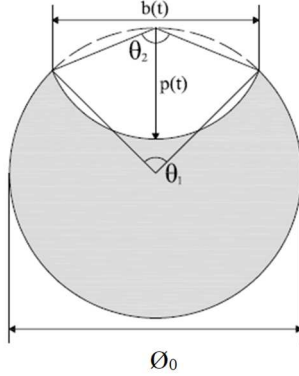


Figure 1. Pitting corrosion model for a corroded reinforcement.

If the pits are assumed of hemispherical shape (Fig.1), the corroded area can be evaluated as:

$$A_{corr}(t) = \left[\frac{\phi_0^2}{8} \cdot (\theta_1(t) - \sin(\theta_1(t))) \right] + \left[\frac{p(t)^2}{2} \cdot (\theta_2(t) - \sin(\theta_2(t))) \right] \quad (4)$$

and the mass loss in the time can be defined as:

$$\%M_{corr}(t) = \left(1 - \frac{A_{corr}(t)}{A_0} \right) \cdot 100 \quad (5)$$

Then, the reinforcement mechanical properties decay due to a certain pitting attack can be easily computed as (Imperatore et al., 2017):

$$\frac{\sigma_{y,corr}(t)}{\sigma_{y,uncorr}} = 1 - 0.019961 \cdot \%M_{corr}(t) \quad (6)$$

$$\frac{\sigma_{u,corr}(t)}{\sigma_{u,uncorr}} = 1 - 0.018642 \cdot \%M_{corr}(t) \quad (7)$$

$$\frac{\varepsilon_{u,corr}(t)}{\varepsilon_{u,uncorr}} = e^{1-0.0546993 \cdot \%M_{corr}(t)} \quad (8)$$

The previous relationships allow defining the corrosion evolution over time as a function of the specific environmental conditions. Once an appropriate knowledge of the structure is acquired, the corrosion propagation by chloride attack can be estimated and related to the nominal life of the structure. By contrast, defining the maximum degradation level of a structure (i.e. as a function of the seismic capacity reduction), the residual structural life can be estimated once the timing of corrosion initiation and propagation has been properly defined.

3 CASE STUDY

The present study analyzes the seismic performance of the structure represented in Figure 2, characterized by a concrete with an average compressive cubic strength of 25 MPa and a reinforcement with a yielding strength of 370 MPa, and an ultimate stress and strain of 545 MPa and 26%, respectively.

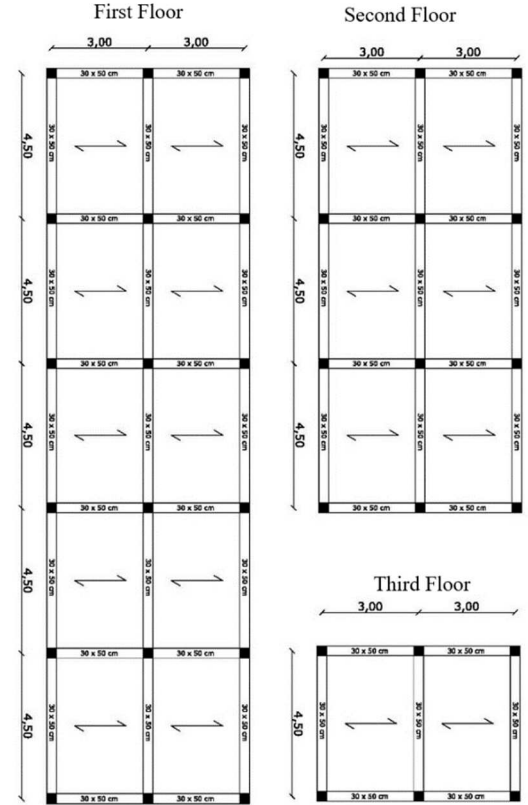


Figure 2. Structural plane of the analyzed building.

All the beams present a 30x50cm² cross-section, with 8mm-diameter stirrups with spacing of 30cm and 14mm-diameter longitudinal reinforcements; three upper bars and two lower bars are placed at the supports, or two upper bars and three lower bars in the mid-span. The columns, all characterized by a 30x30cm² cross-section, are reinforced by 4Ø14 bars if externally disposed, or 8Ø14 bars in the case of internal column; in both the cases 8mm-diameter stirrups, with spacing of 30cm, are ever disposed.

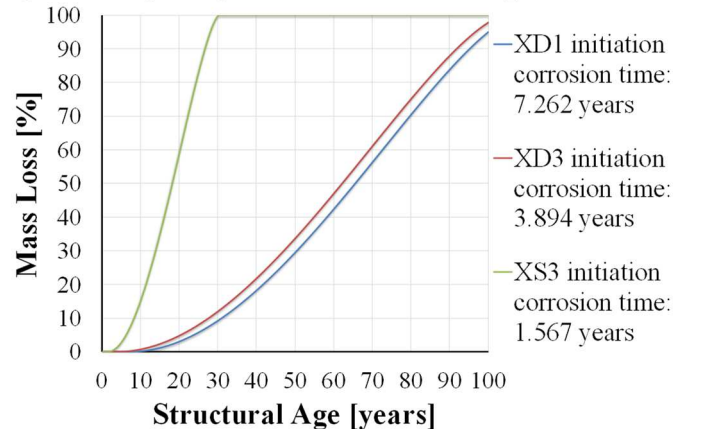


Figure 3. Dependence of the percentage of corrosion at the exposure time.

In Figure 3, the trends over time of the mass loss of reinforcement due to the corrosion are represented for different exposure classes according to EN206. According to (Rodriguez et al., 2006), the analysis is effected by assuming an equivalent corrosion current density between 0.4 and $7 \mu\text{A}/\text{cm}^2$. In order to account the ratio between maximum and minimum pit penetration, the pitting parameter is fixed equal to 6.

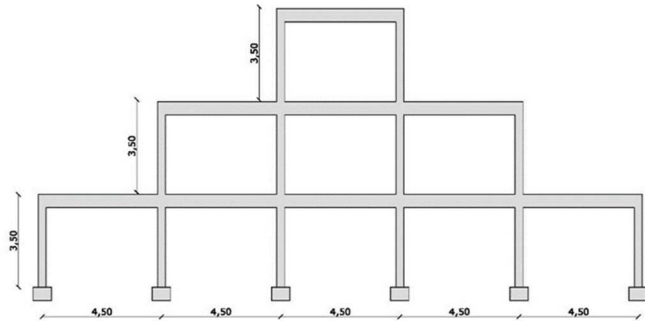


Figure 4. Structural schematization of the irregular frame.

The pushover analyses were performed on a plane model implemented in Seismostruct software, see Fig. 4. Each inelastic element was modeled according to a force-based formulation characterized by the distributed plasticity approach. The concrete was modeled according to the classic Mander relationship, taking into account the confinement induced by the stirrups; for reinforcement, the classic Menegotto-Pinto law has been employed.

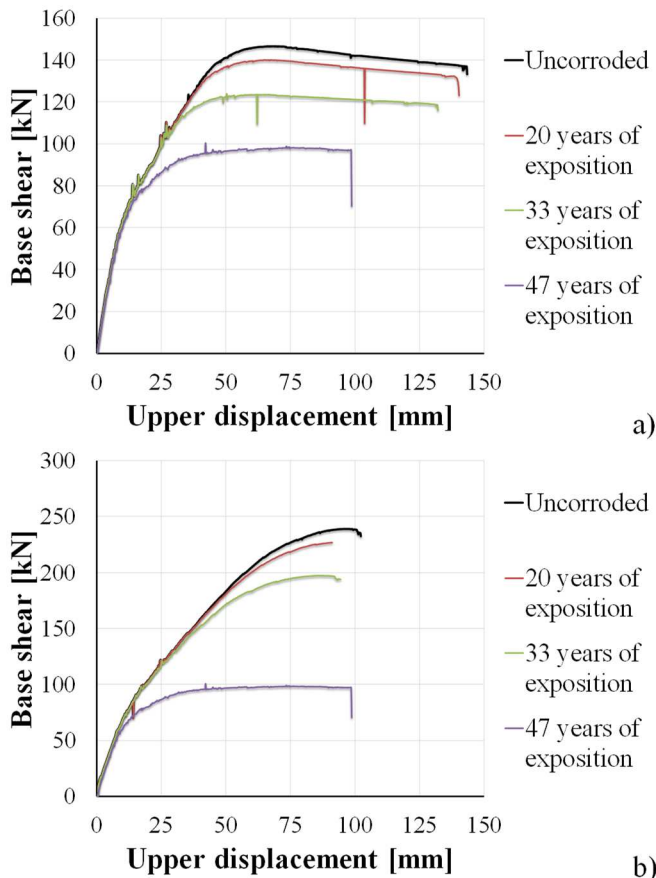


Figure 5. Capacity curves for the entirely corroded frame varying the exposure time in XD3 class: a) live load of 13.7 kN/m ; b) live load of 21.2 kN/m .

Two different load conditions were considered, consisting in a live load of 13.7 kN/m or 21.2 kN/m on each beam. For both conditions, the uncorroded frame is characterized by the formation of a soft-storey at the ground floor. The structure, in fact, was intentionally under-designed for the seismic loads. Due to this peculiarity, all the possible degradation scenarios result in a similar seismic performance.

The corrosion on both longitudinal reinforcement and stirrups is introduced by means of the Equations 6-8 which modify the mechanical properties of steel accounted for also reinforcement cross-section reduction. Consequently, the confinement varies according to the corrosion level. For sake of brevity, only the results obtained for XD3 exposure class are reported.

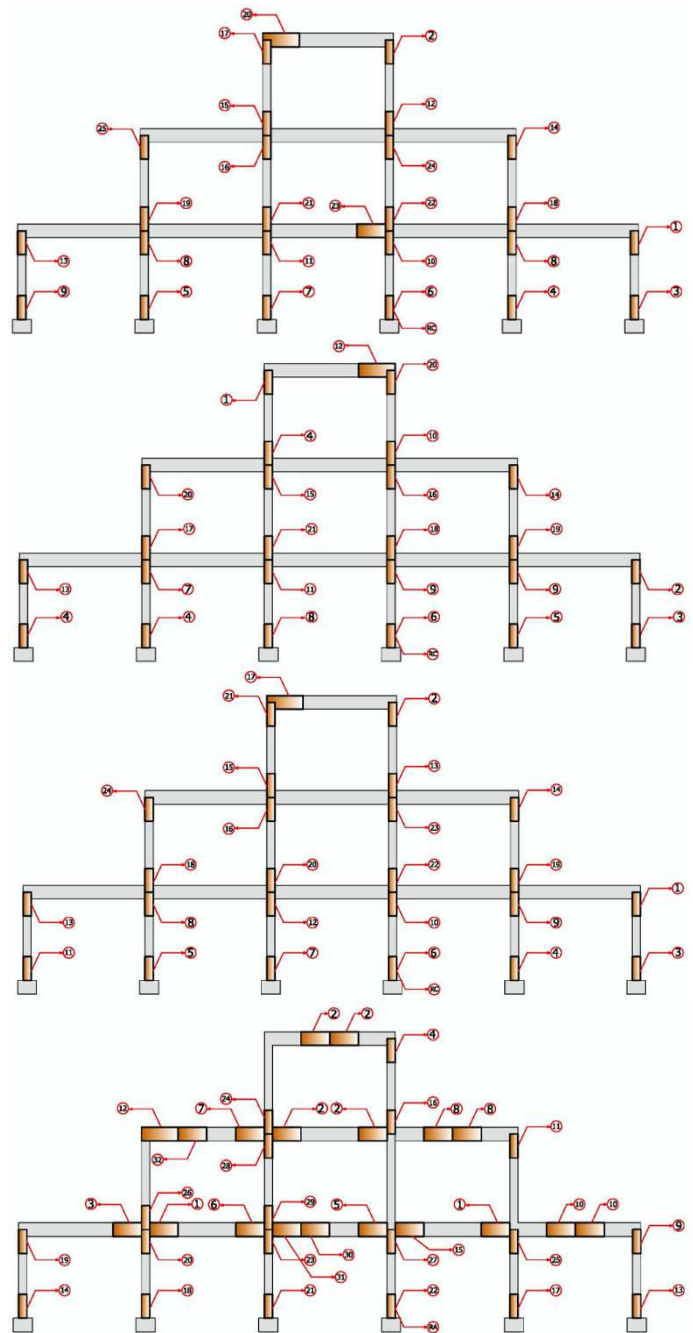


Figure 6. Plastic hinge formation sequence for live load of 13.7 kN/m at different exposition times in XD3 class. From the top: uncorroded (reference), 20 years of exposition, 33 years of exposition, 47 years of exposition.

The obtained results are presented in Figure 5, where the capacity curves for the entirely corroded frames are represented. The structural decay is clear: the strength capacity decreases up to the 50%, while the displacement capacity appears less affected by corrosion due to the fragile seismic behavior of the reference structure. The capacity decay is related to a substantial variation of the plasticization sequence of the structural elements as well as the number of sections involved; in Figures 6-7 the plastic hinge formation sequence at the different exposition times is represented for both the vertical load conditions.

4 CONCLUSIONS

In RC structures, chlorides are a frequent cause of corrosion. The application of the Fick's law and other literature formulations able to evaluate pitting attack as a function of environmental conditions, lead to the definition of a relationship between the pitting corrosion and the exposure time. The latter can be applied to existing structures in order to evaluate the eventual degradation level, to define the residual life of the structure as a function of the maximum tolerable performance reduction, and eventually estimate the seismic performance in the actual conditions.

In the present study, the seismic performance of an irregular under-designed existing structure is analyzed. Due to the formation of a soft-storey at the ground floor in the reference (uncorroded) conditions, all the possible degradation scenarios result in a similar seismic performance. For sake of brevity, only the effects of an exposition to a XD3 class are here reported: in this common environmental condition, for element characterized by a 30mm concrete cover and 14mm-diameter reinforcements, the 35% of mass loss is estimated after an exposition of 50 years (the service life of the structure). The obtained results show a progressive and almost linear structural decay, with dangerous effects after 47 years of exposition, when for low seismic loads all the elements suddenly yield and the structure collapses for the crushing of the confined concrete in the base columns.

5 REFERENCES

- Adam, J. M., Moreno, J. D., Bonilla, M., & Pellicer, T. M. (2016). Classification of damage to the structures of buildings in towns in coastal areas. *Engineering Failure Analysis*, 70, 212-221.
- Andrade, C., Alonso, C., & Molina, F. J. (1993). Cover cracking as a function of bar corrosion: Part I-Experimental test. *Materials and structures*, 26(8), 453-464.
- Andrade, C., Alonso, C., & Sarría, J. (2002). Corrosion rate evolution in concrete structures exposed to the atmosphere. *Cement and concrete composites*, 24(1), 55-64.
- Apostolopoulos, C. A., Demis, S., & Papadakis, V. G. (2013). Chloride-induced corrosion of steel reinforcement—Mechanical performance and pit depth analysis. *Construction and Building Materials*, 38, 139-146.
- Apostolopoulos, C. A., & Papadopoulos, M. P. (2007). Tensile and low cycle fatigue behavior of corroded reinforcing steel bars S400. *Construction and Building Materials*, 21(4), 855-864.
- Baiocchi, V., Dominici, D., Giannone, F., & Zucconi, M. (2012). Rapid building damage assessment using EROS B data: the case study of L'Aquila earthquake. *Italian Journal of Remote Sensing/Rivista Italiana di Telerilevamento*, 44(1).
- Berto, L., Saetta, A., & Simioni, P. (2012). Structural risk assessment of corroding RC structures under seismic excitation. *Construction and building materials*, 30, 803-813.

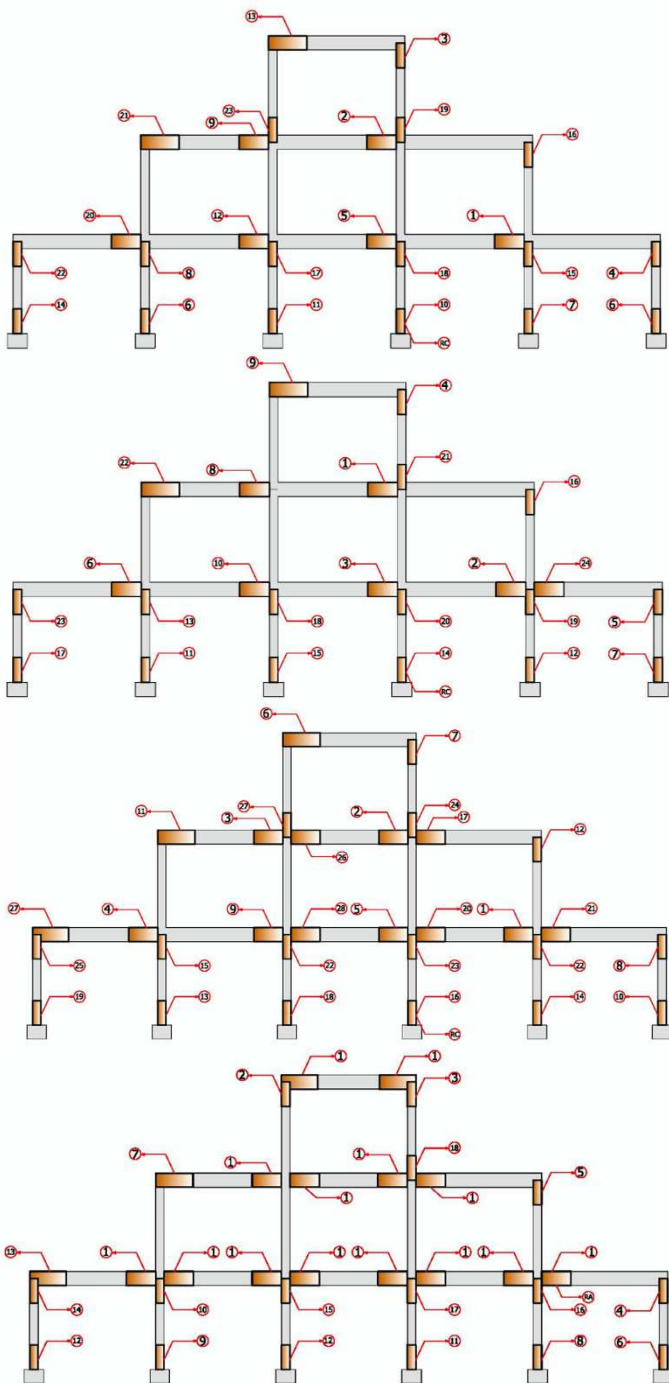


Figure 7. Plastic hinge formation sequence for live load of 21.2 kN/m at different exposition times in XD3 class. From the top: uncorroded (reference), 20 years of exposition, 33 years of exposition, 47 years of exposition.

- Bossio, A., Monetta, T., Bellucci, F., Lignola, G. P., & Prota, A. (2015). Modeling of concrete cracking due to corrosion process of reinforcement bars. *Cement and concrete research*, 71, 78-92.
- Bossio, A., Lignola, G. P., Fabbrocino, F., Monetta, T., Prota, A., Bellucci, F., & Manfredi, G. (2017). Nondestructive assessment of corrosion of reinforcing bars through surface concrete cracks. *Structural Concrete*, 18(1), 104-117.
- Bossio, A., Lignola, G. P., & Prota, A. (2018). An overview of assessment and retrofit of corroded reinforced concrete structures. *Procedia Structural Integrity*, 11, 394-401.
- Bossio, A., Fabbrocino, F., Monetta, T., Lignola, G. P., Prota, A., Manfredi, G., & Bellucci, F. (2019). Corrosion effects on seismic capacity of reinforced concrete structures. *Corrosion Reviews*, 37(1), 45-56.
- Bossio, A., & Bellucci, F. (2019). Environmental degradation of reinforced concrete structures. *Corrosion Reviews*, 37(1), 1-2.
- Coccia, S., Imperatore, S., & Rinaldi, Z. (2016). Influence of corrosion on the bond strength of steel rebars in concrete. *Materials and structures*, 49(1-2), 537-551.
- Coronelli, D. (2002). Corrosion cracking and bond strength modeling for corroded bars in reinforced concrete. *Structural Journal*, 99(3), 267-276.
- de Rincón, O. T., Sánchez, M., Millano, V., Fernández, R., de Partidas, E. A., Andrade, C., ... & Montenegro, J. C. (2007). Effect of the marine environment on reinforced concrete durability in Iberoamerican countries: DURACON project/CYTED. *Corrosion Science*, 49(7), 2832-2843.
- Ferlito, R., Guarascio, M., & Zucconi, M. (2013). Assessment of a vulnerability model against post-earthquake damage data: the case study of the historic city centre of L'Aquila in Italy. *Earthquake Resistant Engineering Structures IX*, 132, 393.
- fib (2006): "Model Code for Service Life Design", Bulletin 34
- Kashani, M. M., Crewe, A. J., & Alexander, N. A. (2013). Non-linear cyclic response of corrosion-damaged reinforcing bars with the effect of buckling. *Construction and Building Materials*, 41, 388-400.
- Kashani, M. M., Crewe, A. J., & Alexander, N. A. (2013). Non-linear stress-strain behaviour of corrosion-damaged reinforcing bars including inelastic buckling. *Engineering Structures*, 48, 417-429.
- Kioumarsis, M. M., Hendriks, M. A., & Geiker, M. R. (2014). Quantification of the interference of localised corrosion on adjacent reinforcement bars in a concrete beam in bending. *Nordic Concrete Research (NCR)*, 49, 39-57.
- Kioumarsis, M., Hendriks, M. A., & Geiker, M. (2015). Failure probability of a corroded beam with interference effect of localised corrosion. *Nordic Concrete*, 39.
- Kioumarsis, M. M., Hendriks, M. A., Kohler, J., & Geiker, M. R. (2016). The effect of interference of corrosion pits on the failure probability of a reinforced concrete beam. *Engineering Structures*, 114, 113-121.
- Kioumarsis, M., Markeset, G., & Hooshmandi, S. (2017). Effect of pit distance on failure probability of a corroded RC beam. *Procedia Engineering*, 171, 526-533.
- Inci, P., Goksu, C., Ilki, A., & Kumbasar, N. (2012). Effects of reinforcement corrosion on the performance of RC frame buildings subjected to seismic actions. *Journal of Performance of Constructed Facilities*, 27(6), 683-696.
- Imperatore, S., Leonardi, A., & Rinaldi, Z. (2012). Mechanical behaviour of corroded rebars in reinforced concrete elements. In *Mechanics, Models and Methods in Civil Engineering* (pp. 207-220). Springer, Berlin, Heidelberg.
- Imperatore, S., Leonardi, A., & Rinaldi, Z. (2016). Strength decay of RC sections for chloride attack. *International Journal of Structural Integrity*, 7(2), 194-212.
- Imperatore, S., Rinaldi, Z., & Drago, C. (2017). Degradation relationships for the mechanical properties of corroded steel rebars. *Construction and Building Materials*, 148, 219-230.
- Lindvall, A. (2007). Chloride ingress data from field and laboratory exposure—Influence of salinity and temperature. *Cement and Concrete Composites*, 29(2), 88-93.
- Liu, Y., & Weyers, R. E. (1996). Time to cracking for chloride-induced corrosion in reinforced concrete. *Special Publications of the Royal Society of Chemistry*, 183, 88-104.
- Liu, T., & Weyers, R. W. (1998). Modeling the dynamic corrosion process in chloride contaminated concrete structures. *Cement and Concrete Research*, 28(3), 365-379.
- Medeiros, M. H. F., Gobbi, A., Réus, G. C., & Helene, P. (2013). Reinforced concrete in marine environment: Effect of wetting and drying cycles, height and positioning in relation to the sea shore. *Construction and Building Materials*, 44, 452-457.
- Meira, G. R., Andrade, C., Alonso, C., Padaratz, I. J., & Borba, Z. J. (2008). Modelling sea-salt transport and deposition in marine atmosphere zone—A tool for corrosion studies. *Corrosion Science*, 50(9), 2724-2731.
- Meira, G. R., Pinto, W. T. A., Lima, E. E. P., & Andrade, C. (2017). Vertical distribution of marine aerosol salinity in a Brazilian coastal area—The influence of wind speed and the impact on chloride accumulation into concrete. *Construction and Building Materials*, 135, 287-296.
- Moreno, J. D., Bonilla, M., Adam, J. M., Borrachero, M. V., & Soriano, L. (2015). Determining corrosion levels in the reinforcement rebars of buildings in coastal areas. A case study in the Mediterranean coastline. *Construction and Building Materials*, 100, 11-21.
- Rodriguez, J., Ortega, L. M., & Casal, J. (1997). Load carrying capacity of concrete structures with corroded reinforcement. *Construction and building materials*, 11(4), 239-248.
- Rodriguez, J., Ortega, L., Izquierdo, D., & Andrade, C. (2006). Calculation of structural degradation due to corrosion of reinforcements. In *Measuring, Monitoring and Modeling Concrete Properties* (pp. 527-536). Springer, Dordrecht.
- Romano, F., Faggella, M., Gigliotti, R., Zucconi, M., & Ferracuti, B. (2018). Comparative seismic loss analysis of an existing non-ductile RC building based on element fragility functions proposals. *Engineering Structures*, 177, 707-723.
- Vidal, T., Castel, A., & Francois, R. (2004). Analyzing crack width to predict corrosion in reinforced concrete. *Cement and concrete research*, 34(1), 165-174.
- Vidal, T., Castel, A., & Francois, R. (2007). Corrosion process and structural performance of a 17 year old reinforced concrete beam stored in chloride environment. *Cement and Concrete Research*, 37(11), 1551-1561.
- Val, D. V., & Melchers, R. E. (1997). Reliability of deteriorating RC slab bridges. *Journal of structural engineering*, 123(12), 1638-1644.
- Vu, K. A. T., & Stewart, M. G. (2000). Structural reliability of concrete bridges including improved chloride-induced corrosion models. *Structural safety*, 22(4), 313-333.
- Zhang, R., Castel, A., & François, R. (2010). Concrete cover cracking with reinforcement corrosion of RC beam during chloride-induced corrosion process. *Cement and Concrete Research*, 40(3), 415-425.
- Zandi Hanjari, K., Kettl, P., & Lundgren, K. (2011). Analysis of mechanical behavior of corroded reinforced concrete structures. *ACI Structural Journal*, 108(5), 532-541.
- Zanini, M. A., Faleschini, F., & Pellegrino, C. (2017). Probabilistic seismic risk forecasting of aging bridge networks. *Engineering Structures*, 136, 219-232.
- Zanini, M. A., Faleschini, F., & Pellegrino, C. (2016). Cost analysis for maintenance and seismic retrofit of existing bridges. *Structure and Infrastructure Engineering*, 12(11), 1411-1427.